Cambridge Centre for Computational Chemical Engineering

University of Cambridge

Department of Chemical Engineering

Preprint ISSN 1473 – 4273

A New Computational Model for Simulating Direct Injection HCCI Engines

Haiyun Su, Alexander Vikhansky, Sebastian Mosbach, Markus Kraft [1], Amit Bhave[2], Fabian Mauss [3] and Kyoung-Oh Kim [4]

submitted: October 14, 2005

[1] Department of Chemical Engineering
University of Cambridge
Pembroke Street
Cambridge CB2 3RA
UK
E-mail: mk306@cam.ac.uk

[2] Reaction Engineering Solutions Ltd.
61 Canterbury Street
Cambridge CB4 3QG
UK
E-mail: amitbhave@resolutionsltd.com

[3] Division of Combustion Physics
Lund Institute of Technology
Box 118, S-221 00 Lund
Sweden
E-mail: fabian.mauss@forbrf.lth.se

[4] Higashifuji Technical Center
TOYOTA Motor Corporation
Mishuku 1200, Susono, Shizuoka
JAPAN, 480-1193
E-mail: kim@k.tec.toyota.co.jp

Preprint No. 31

c4e

Key words and phrases. HCCI, SRM, direct injection.

Edited by
Cambridge Centre for Computational Chemical Engineering
Department of Chemical Engineering
University of Cambridge
Cambridge CB2 3RA
United Kingdom.

Fax: + 44 (0)1223 334796
E-Mail: c4e@cheng.cam.ac.uk
World Wide Web: http://www.cheng.cam.ac.uk/c4e/

Abstract

We present a new probability density function (PDF) based computational model to simulate a direct injection (DI) homogeneous charge compression ignition (HCCI) engine. This stochastic reactor model (SRM) accounts for the engine breathing process in addition to the closed-volume HCCI engine operation. A weighted-particle Monte Carlo method is used to solve the resulting PDF transport equation. While simulating the gas exchange, it is necessary to add a large number of stochastic particles to the ensemble due to the intake air and EGR streams as well as fuel injection, resulting in an increased computational expense. Therefore, in this work we apply a down-sampling technique in order to reduce the number of stochastic particles, while conserving the statistical properties of the ensemble. In this method some of the most important statistical moments (e.g., concentration of the main chemical species and enthalpy) are conserved exactly, while other moments are conserved in a statistical sense. Detailed analysis demonstrates that the statistical error associated with the down-sampling algorithm is more sensitive to the number of particles than to the number of conserved species for the given operating conditions. For a full-cycle simulation this down-sampling procedure was observed to reduce the computational time by a factor of eight as compared to the simulation without this strategy, whilst still maintaining the error within an acceptable limit. Furthermore, the new model is applied to qualitatively estimate the influence of engine parameters such as the relative air-fuel ratio and injection timing on HCCI combustion and emissions.

Contents

Nomenclature

Abbreviations

BDC Bottom Dead Centre

CAD Crank Angle Degree

CFD Computational Fluid Dynamics

DI Direct Injection

EOI End of Injection

EVC Exhaust Valve Closing

EVO Exhaust Valve Opening

HCCI Homogeneous Charge Compression Ignition

IEM Interaction by Exchange with the Mean model

IVC Intake Valve Closing

IVO Intake Valve Opening

MDF Mass Density Function

PDF Probability Density Function

PaSR Partially Stirred Reactor

SOI Start of Injection

SRM Stochastic Reactor Model

SRM-DI Stochastic Reactor Model for Direct Injection

TDC Top Dead Centre

TRG Trapped Residual Gas

FP Number of inflowing fuel particles per time step

LB Lower Bound

RS Random Seed

UB Upper Bound

c Engine cycle index

Roman Symbols

C_ϕ	Proportionality constant of the IEM model
C_{stat}	Statistical error
C_{sys}	Systematic error
$F(t)$	Reference solution
I_p	Confidence interval
L	Number of simulation repetitions
M	Down-sampling factor, $M = \frac{N}{n}$
M_{tot}	Total mass
N	Number of particles before down-sampling
N_{a}	Number of air particles added to the ensemble per step
N_{f}	Number of fuel particles added to the ensemble per step
$W^{(i)}$	Statistical weight of particle
W_{max}	Maximum statistical weight
Z	A linear functional of mass density function
$\dot{m}$	Mass flow rate
g	A uniformly distributed unit vector
n	Number of particles after down-sampling
ns	Number of conserved species
s	Number of species
t	Time
z	An integrable function
$\mathcal{F}$	Mass density function

Greek Symbols

Π_{ji}	Matrix of particle weights

α_p Confidence coefficient

δ Delta function

ψ Scalar variables

τ_a, τ_e, τ_f Air, exhaust and fuel residence times

τ_m Mixing time

$\zeta^{n,l}(t)$ Macroscopic properties

$\eta_1^{n,L}$ Empirical mean value of macroscopic properties for L repetitions

η_1^n Empirical mean value of scalar variables for n particles

$\eta_2^{n,L}$ Empirical variance of macroscopic properties for L repetitions

η_2^n Empirical variance of scalar variables for n particles

Subscripts/Superscripts

$^{\text{in}}$ Inflow

$^{\text{out}}$ Outflow

$_{\text{a}}$ Air

$_{\text{e}}$ Exhaust gas

$_{\text{f}}$ Fuel

$_{\text{m}}$ Mixing

1 Introduction

The development of efficient internal combustion engines with ultra-low emissions is necessitated by strict regulations on exhaust gas composition and fuel economy. Homogeneous charge compression ignition (HCCI) technology, incorporating the advantages of both spark ignition and compression ignition, is a potential candidate for future ultra-low emission engine strategies. There are, however, technical hurdles to overcome before large scale production and application of HCCI engines can be achieved. Further research and development needs to be conducted in order to control HCCI combustion and expand the engine operating window. Various approaches such as multiple direct injections, variable valve timing, dual fuels, variable compression ratio and intake charge heating have shown potential to tackle the above mentioned issues (Zhao et al., 2003).

In particular, direct injection (DI) has been widely investigated to control the spontaneous combustion as well as to expand the engine operating region. Optimum values for single direct injection timings have been demonstrated under different operating load conditions, and have been shown to be capable of expanding the lean limit by promoting better fuel ignitability (Urushihara et al., 2003; Standing et al., 2005). Early injection timing results in a more homogeneous mixture, and it can lead to thermodynamically unfavorable advanced combustion timing under high load (Guenthner et al., 2004; Leach et al., 2005). To help control ignition timing and combustion duration, a dual-injection strategy has been investigated (Guenthner et al., 2004; Hasegawa and Yanagihara, 2003). The second fuel injection can function as an ignition trigger and can help to limit pressure rise rates caused by too rapid combustion. Elsewhere, in order to increase the mixing efficiency and expand operation limit, a number of methods were studied to control the direct injection procedure such as varying injection pressure, spray angle, spray shape and using impingement spray (Tao et al., 2005; Ra and Reitz, 2005; Lechner et al., 2005; Nishijima et al., 2002; Tomoda et al., 2001). Furthermore, Su et al. (Su et al., 2005) have evaluated the effects of pulse injection modes on the suppression of wall wetting.

To evaluate these strategies, computational modelling tools can provide significant insight in a cost- and time-effective manner. A combined single zone and multi-zone based engine cycle model has been introduced for modelling early DI HCCI operation (Narayanaswamy and Rutland, 2004). In their subsequent study, this approach was further improved by incorporating a refined grid to resolve the early spray evolution and a coarse grid when chemical kinetics became prominent (Narayanaswamy et al., 2005). In another study, the influence of air-fuel distribution and temperature distribution on the ignition dwell in an early DI HCCI engine has been modelled using a KIVA 3V code (Jhavar and Christopher, 2005). It was demonstrated that, at the end of fuel injection, the ignition dwell duration was more sensitive to the in-cylinder temperature distribution than the air-fuel distribution. However, these modelling approaches have been limited to early direct injection, and further development for modelling multiple injection and late direct injection HCCI is required.

Probability density function (PDF) based models provide a sophisticated approach while including detailed chemistry and accounting for inhomogeneities in composition and temperature. As special cases, stochastic reactor models (SRMs) are derived from the PDF transport equations assuming statistical homogeneity. The closed volume SRM has been demonstrated to accurately predict auto-ignition timing, in-cylinder pressure and emissions in HCCI engines (Kraft et al., 2000; Maigaard et al., 2003; Bhave et al., 2004a). The model has also been coupled with a commercial code to enable multiple engine cycle simulation (Bhave et al., 2004b, 2005). In previous works, the SRM has been applied to simulate port fuel injected HCCI engines. The present work is the first step of development of an advanced SRM-DI model capable of simulating multiple direct injection HCCI combustion and emissions. This advancement entails the modelling of the engine breathing processes in the existing SRM framework, thus accounting for the detailed chemical kinetics particularly during multiple and late direct injections.

The **aims of this paper** are the following:

1. To develop a new SRM-DI to account for gas exchange and compression-combustion-expansion in a direct injection HCCI engine, such that detailed chemistry can be accounted for during the direct injection process.

2. To formulate a weighted-particle Monte Carlo method in order to solve the transport equation including the gas exchange terms. As compared to the equi-weighted method used in previous works (Bhave et al., 2004a,b, 2005), a weighted-particle method requires fewer particles to account for the gas exchange process.

3. To incorporate a novel down-sampling algorithm to reduce the number of particles in the ensemble (Vikhansky and Kraft, 2005). A number of new particles are added into the system during the air intake and fuel injection, which results in a dramatic increase in the computational cost for the following cycle. In this work, a down-sampling algorithm is employed to reduce the number of particles while conserving the most important statistical properties of the ensemble.

4. To apply the new SRM-DI to predict the qualitative trends, associated with some engine parametric variation, such as varying air-fuel ratio and early DI timing to test the capability of the model to simulate early DI HCCI engines.

This paper is organized as follows. In the second section, the sub-models for the DI HCCI engine are described. In section 3, the numerical method and its implementation are presented. In section 4, an error analysis is conducted to determine appropriate down-sampling parameters, by studying the statistical errors associated with the procedure. Then, multiple cycle simulations were performed to test if the error due to down-sampling was accumulated in subsequent engine cycles. Furthermore, the effect of the down-sampling procedure in terms of computational gains

and accuracy are evaluated by comparing the in-cylinder temperature and chemical species obtained with and without this technique. Two cases, "well-mixed" and "partially mixed", are investigated. In section 5, the SRM-DI is applied to study the effects of air-fuel ratio and early direct injection timing on the combustion and emissions in a DI HCCI engine. Conclusions are drawn in the final section and future work is discussed.

2 SRM for Direct Injection HCCI

The partially stirred reactor (PaSR) model has been widely used as a test bed for evaluating chemical mechanisms and mixing schemes in the field of combustion (Correa and Braaten, 1993; Chen, 1997; Bhave and Kraft, 2004). This model assumes statistical homogeneity of the mixture in the reactor. It accounts for mixing and is computationally efficient for large coupled chemical reaction mechanisms.

In this study, we develop a stochastic reactor model on the basis of the PaSR to simulate a direct injection HCCI engine. DI HCCI involves an early injection of fuel into a mixture of air and trapped residual gas (TRG) followed by compression and auto-ignition. This model is denoted as to stochastic reactor model for direct injection (SRM-DI), and can be written as

$$\begin{aligned}
&\tfrac{\partial}{\partial t}\mathcal{F}(\psi,t) + \underbrace{\frac{1}{V}\frac{dV}{dt}\mathcal{F}(\psi,t)}_{\text{piston movement}} + \underbrace{\sum_{i=1}^{s+1}\frac{\partial}{\partial\psi_i}\left[G_i(\psi)\mathcal{F}(\psi,t)\right]}_{\text{chemical kinetics}} \\
&\quad + \underbrace{\frac{1}{h}[U(\psi_{s+1}+h)\mathcal{F}(\psi_1,...,\psi_s,\psi_{s+1}+h,t) - U(\psi_{s+1})\mathcal{F}(\psi,t)]}_{\text{convective heat transfer}} \\
&= \underbrace{\sum_{i=1}^{s+1}\frac{\partial}{\partial\psi_i}\left[\frac{C_\phi}{2\tau_{\mathrm{m}}}(\psi(t)-\langle\psi_i\rangle)\mathcal{F}(\psi,t)\right]}_{\text{mixing}} + \underbrace{\frac{{}_{\mathrm{a}}\mathcal{F}_{\mathrm{in}}(\psi,t)}{\tau_{\mathrm{a}}} - \frac{\mathcal{F}(\psi,t)}{\tau_{\mathrm{e}}} + \frac{{}_{\mathrm{f}}\mathcal{F}_{\mathrm{in}}(\psi,t)}{\tau_{\mathrm{f}}}}_{\text{gas exchange and fuel injection}}
\end{aligned} \tag{1}$$

with the initial condition

$$\mathcal{F}(\psi,0) = \mathcal{F}_0(\psi), \tag{2}$$

where $\mathcal{F}$ is the mass density function (MDF), ψ stands for scalar variables such as mass fractions of chemical species and temperature, i.e. $\psi = (\psi_1,...,\psi_s,\psi_{s+1}) = (Y_1,...,Y_s,T)$. The five terms accounting for piston movement, chemical kinetics and volume change, convective heat transfer, mixing, gas exchange and fuel injection respectively (as indicated in eqn. (1)) are now described in more detail.

The second term on the left hand side (LHS) of eqn. (1) denotes the effect of the piston movement on the MDF. The chemical kinetics and the energy associated with the change in volume is represented by the third term on the LHS where,

$$G_i = \frac{M_i\dot{\omega}_i}{\rho}, \qquad i = 1,\ldots,s, \tag{3}$$

$$G_{s+1} = -\frac{1}{\rho c_{\mathrm{v}}} \sum_{i=1}^{s} e_i M_i \dot{\omega}_i - \frac{p}{m c_{\mathrm{v}}} \frac{dV}{dt}. \tag{4}$$

Here, M_i is the molar mass of species i, ρ is the density of the mixture, $\dot{\omega}_i$ is the molar production rate of the i^{th} species, V is the volume, m is the mass and e_i represents the specific internal energy of species i. In this paper, a deterministic solver based on a backward differentiation formula method was implemented to solve the set of stiff ordinary differential equations.

The fourth term on the LHS of eqn. (1) represents the heat transfer model, where h denotes the fluctuation (the implementation is discussed in section 3.1),

$$U(T) = -\frac{h_g A}{c_{\mathrm{v}} M_{\mathrm{tot}}} (T - T_{\mathrm{W}}), \tag{5}$$

and h_g is the Woschni heat transfer coefficient, A is the heat transfer area, M_{tot} is the total mass, c_{v} is the specific heat capacity at constant volume and T_{W} denotes the wall temperature. Heat transfer occurs between the fluid and the wall due to convection. It is modelled as a stochastic jump process based on the Woschni heat transfer coefficient (Bhave et al., 2004a, 2005).

For mixing, the interaction by exchange with the mean (IEM) model, represented by the first term on the right hand side (RHS) of eqn. (1), was used. The IEM model (also known as linear mean square estimation (LMSE) model) is a deterministic model whose main features are simplicity and low computational effort. The model works on the principle that the scalar value at a point approaches the mean scalar value over the entire volume with a characteristic time τ_m. For a single scalar, the IEM model is given by:

$$\frac{d\psi(t)}{dt} = -\frac{C_\phi}{2\tau_m} (\psi(t) - \langle \phi \rangle) \tag{6}$$

where C_ϕ is a model constant. In this paper, C_ϕ is set to 2.0 as suggested by Pope (1985).

On the RHS of eqn. (1), last three terms account for the gas exchange process in DI HCCI (air intake, exhaust and fuel injection). τ_{a}, τ_{e}, τ_{f} denote the characteristic residence times of air, exhaust gas and fuel respectively. ${}_{\mathrm{a}}\mathcal{F}_{\mathrm{in}}$, ${}_{\mathrm{f}}\mathcal{F}_{\mathrm{in}}$ stand for mass density function associated with the intake air and fuel streams.

3 Numerical method

In this section, the numerical method employed for the solution of eqn. (1) is discussed in detail. A weighted-particle Monte Carlo method with an operator splitting procedure has been implemented in this work.

The particle method involves representation of the reactive system by a notional ensemble of N particles. Thus the approximation for the mass density function $\mathcal{F}$ reads:

$$\mathcal{F}(\psi,t) = \rho(\psi,t)f(\psi,t) \approx \frac{\rho(\psi,t)}{\sum_{i=1}^{N} W^{(i)}} \sum_{i=1}^{N} W^{(i)}\delta(\psi - \psi^{(i)}(t)) = \frac{1}{V(t)} \sum_{i=1}^{N} W^{(i)}\delta(\psi - \psi^{(i)}(t)). \tag{7}$$

where W_i is the weight of the i^{th} particle.

Therefore,

$$\langle\rho(t)\rangle = \int \rho(\psi,t)f(\psi,t)d\psi = \int \mathcal{F}(\psi,t)d\psi = \frac{1}{V(t)} \sum_{i=1}^{N} W^{(i)} = \frac{M_{\text{tot}}}{V(t)} \tag{8}$$

Following this approximation $\mathcal{F}_0(\psi) \approx \frac{1}{V_0} \sum_{i=1}^{N} W_0^{(i)}\delta(\psi - \psi_0^{(i)})$, each particle is moved according to the evolution of the mass density function eqn. (1).

The operator splitting technique is used to simplify an evolution equation by splitting the complex equation into a set of equations. The advantage is that the splitted equations can be treated separately at the expense of introducing a splitting error. The operator splitting technique was discussed in detail by (Strang, 1968), and has been applied to the PDF transport equation by Pope (Pope, 1985). It has been demonstrated that the splitting is first order accurate (Yang and Pope, 1998).

In the previous work (Bhave et al., 2004a,b, 2005), equi-weighted particle method was used. In this work, a weighted-particle method is employed so that it can be directly coupled with the down-sampling procedure. The implementation of the chemical kinetics, mixing and heat transfer models are readily generalized to weighted-particle systems since they are independent of the statistical weight.

3.1 Implementation of SRM-DI

Based on the numerical method described above, the SRM-DI was implemented as follows:

1: Initialize $t = 0, t_{\text{stop}}, \Delta t$, CAD (Crank Angle Degree) = IVC (Intake Valve Closing). Determine the state of the particle system at time $t = 0$.

2: Progress in time with a time step, $t \mapsto t + \Delta t$. If $t > t_{\text{stop}}$, then stop. Else, if CAD < EVO (Exhaust Valve Opening) go to step 3, otherwise go to step 8.

3: Perform the mixing step: the particle ensemble is updated according to eqn. (6).

4: Perform the reaction step.

5: Perform the mixing step.

6: Choose particles uniformly and perform the heat transfer step $T^{(i)} \mapsto T^{(i)} - h^{(i)}$, where the fluctuation $h^{(i)} = \frac{T^{(i)} - T_{\mathrm{W}}}{C_h}$ and C_h is a parameter in the model which determines the magnitude of the fluctuation.

7: Go to step 2.

8: Perform the inflow-outflow step, as it is described below.

9: If CAD = IVC perform the down-sampling.

10: Go to step 2.

The inflow-outflow step as given in point 8 above is a new sub-model and is discussed in detail in the next sub-section.

3.2 Implementation of inflow and outflow

In this study, the inflow-outflow model accounts for the following events - intake of fresh air, fuel injection and exhaust.

In an inflow event, fresh air and fuel particles are added to the system, $N \mapsto N + N_{\mathrm{in}}$, where N_{in} denotes the number of new particles added per step (Δt). The weight of a new particle equals its mass, leading to

$$W^{(i)} = \frac{\dot{m}^{\mathrm{in}} \times \Delta t}{N_{\mathrm{in}}}, \qquad i = N+1, \ldots, N+N_{\mathrm{in}}. \tag{9}$$

Here, $\dot{m}^{\mathrm{in}}$ denotes the mass flow rate of the inflow stream.

For outflow we note that the mass to be removed during the time interval Δt is given by $\Delta t\, \dot{m}_{\mathrm{e}}^{\mathrm{out}}$, where $\dot{m}_{\mathrm{e}}^{\mathrm{out}}$ denotes the mass flow rate of the exhaust stream. Hence, the fraction of mass to be removed equals $\dot{m}_{\mathrm{e}}^{\mathrm{out}} / M_{\mathrm{tot}}$. Due to the overlap of the exhaust process and fuel injection, a stochastic method can result in the fluctuation of fuel concentration from cycle to cycle. To tackle this issue, a deterministic method is implemented. We now assume that every mass element has the same probability to be removed (i.e. flowing out of the cylinder), and obtain

$$W^{(i)} \mapsto W^{(i)} \times (1 - \Delta t \frac{\dot{m}_{\mathrm{e}}^{\mathrm{out}}}{M_{\mathrm{tot}}}), \qquad i = 1, \ldots, N. \tag{10}$$

For simplicity, we assume constant inflow and outflow rates throughout. Within a time step $t \leqslant \mathrm{CAD} \leqslant t + \Delta t$ the algorithm is implemented as follows:

1: Given the state at CAD = EVO, initialize $W^{(i)} = W_0^{(i)}$.

2: For EVO $<$ CAD $\leqslant$ EVC (Exhaust Valve Closing), perform an outflow event, i.e., reduce the particle weight $W^{(i)}$ proportionally according to (10).

3: For IVO (Intake Valve Opening) $<$ CAD $\leqslant$ IVC, perform the inflow of fresh air i.e., add N_{a} particles to the ensemble according to eqn. (9), where $\dot{m}_{\mathrm{in}} = \dot{m}_{\mathrm{air}}^{\mathrm{in}}$ and $N_{\mathrm{in}} = N_{\mathrm{a}}$. $\dot{m}_{\mathrm{air}}^{\mathrm{in}}$ denotes the mass flow rate of inflowing air.

4: For SOI (Start of Injection) $<$ CAD $\leqslant$ EOI (End of Injection), perform the inflow event for fuel streams according to eqn. (9) with $\dot{m}_{\text{in}} = \dot{m}^{\text{in}}_{\text{fuel}}$ and $N_{\text{in}} = N_{\text{f}}$. $\dot{m}^{\text{in}}_{\text{fuel}}$ denotes the mass flow rate of injected fuel.

Adding particles to the ensemble causes a significant increase in computational expense. It is necessary to reduce the number of the particles without affecting the statistics of the ensemble. This procedure, called down-sampling, is discussed in the next sub-section.

3.3 Down-sampling algorithm

The simplest method which removes particles chosen according to the uniform distribution from the ensemble, leads to large spurious fluctuations of energy and mass of the chemical species. In this study we apply the method introduced by (Vikhansky and Kraft, 2005) which randomly redistributes the statistical weights between the particles in such a way that the weight of some particles becomes 0 (i.e., the particles are removed), while the most important statistical moments of the ensemble are conserved and overall the ensemble remains statistically unaffected (a more detailed description of the method is given in the Appendix). In the present investigation we chose ns species which, due to their high significance, have to be conserved exactly in addition to conserving the enthalpy of the mixture. The algorithm is implemented as follows:

1: Determine the state of the particle system at time IVC

$$\psi^{(i)}_j,\ W^{(i)},\ t = \text{IVC}, \quad i = 1, \ldots, N,\ j = 1, \ldots, s+1.$$

2: Calculate the average values of all properties $\langle \psi_j \rangle$, and sort them in descending order, where

$$\langle \psi_j \rangle = \frac{\sum\limits_{i=1}^{N} \psi^{(i)}_j \times W^{(i)}}{\sum\limits_{i=1}^{N} W^{(i)}}, \quad i = 1 \ldots N,\ j = 1, \ldots, s+1.$$

3: Choose the first ns species according to $\langle \psi_j \rangle$ and the enthalpy, then calculate the $(N \times (ns+1))$ matrix Π, where

$$\Pi_{ji} = \psi^{(i)}_j,\ i = 1, \ldots, N, \quad j = 1, \ldots, ns+1.$$

4: Set maximum weight $W_{\max}$, and perform the reduction (for reduction algorithm see the Appendix) with parameters Π and $W_{\max}$. Calculate the new statistical weight $W^{(i)}$.

5: Remove all particles satisfying the condition $W^{(i)} < \sum W^{(i)} \times 10^{-5}$. The number of remaining particles n lies in the interval $(\frac{\sum W^{(i)}}{W_{\max}}, \frac{\sum W^{(i)}}{W_{\max}} + ns + 1)$.

4 Numerical Properties of the Algorithm

The SRM-DI discussed above was implemented to simulate a two-stroke, iso-octane fuelled HCCI test engine. The description of the engine and its operating parameters is given in Table 1. In the study, the temperature and the mass fractions of OH, CO,

Table 1: *Engine operating parameters.*

Description	Value	Units
Displaced Volume	1500	cm^3
Bore	86	mm
Stroke	86	mm
Connection rod	154	mm
Speed	1200	RPM
Fuel	iso-octane	–
Compression ratio	13.5	–
EVO/EVC	140/180 ATDC	CAD
IVO/IVC	155/215 ATDC	CAD
SOI/EOI	165/175 ATDC	CAD

and NO_x were considered to represent the scalar variables to be studied for data analysis. Two cases of turbulent mixing, one partially mixed ($\tau_m = 2.0 \times 10^{-2}$ s) and the other well-mixed ($\tau_m = 2.0 \times 10^{-4}$ s) were chosen to represent the extremes of the characteristic mixing times during gas exchange. The mixing time for compression-combustion-expansion is set to $\tau_m = 2.0 \times 10^{-2}$ s. For the well-mixed case even a very simple down-sampling method, for example, obtaining the scalar properties by averaging the properties of all the particles at IVC, matched well with the solution (Bhave et al., 2004b). It is the partially mixed case for which a sophisticated down-sampling method is required. Before investigating the numerical properties of the down-sampling algorithm, the influence of the number of fuel particles added to the system during every step of the direct injection phase is studied in section 4.1. For this sub-section, no down-sampling algorithm was involved, and the partially mixed case was employed for the simulation.

4.1 Influence of the number of inflowing fuel particles

The influence of the number of fuel particles injected into the chamber during every time step (0.3 CAD) on the prediction of combustion parameters and chemical species was investigated in this section. The in-cylinder temperature and mass fractions of CO, nitrogen oxides (NO_x) and OH, were obtained with the number of fuel entering particles being set at 1, 2, 4 and 8. A confidence band, with respect

to the number of particles, for the simulation with one repetition was employed for data analysis.

The empirical mean value of scalar variables, in a single-run simulation, is

$$\eta_1^n(t) = \frac{\sum_{i=1}^{n} \psi^{(i)}(t) W^{(i)}}{\sum_{i=1}^{n} W^{(i)}}, \tag{11}$$

where n represents the number of particles after down-sampling.

The empirical variance is

$$\eta_2^n(t) = \frac{\sum_{i=1}^{n} [\psi^{(i)}(t)]^2 W^{(i)}}{\sum_{i=1}^{n} W^{(i)}} - [\eta_1^n(t)]^2. \tag{12}$$

We use as an estimate for the variation of the empirical mean the following confidence interval I_p,

$$I_p = \left[\eta_1^n(t) - 3.0\sqrt{\frac{\eta_2^n(t)}{n}}, \eta_1^n(t) + 3.0\sqrt{\frac{\eta_2^n(t)}{n}} \right]. \tag{13}$$

The results are summarised in Figure 1. Here, LB and UB denote lower bound and upper bound respectively, and FP denotes the number of inflowing fuel particles per time step.

Figure 1 shows that the simulated results with different numbers of fuel particles added during every step are all within the confidence band, determined based on the situation that the fuel particle number was equal to one. This indicates that the statistical error associated with the scalars (the temperature and mass fractions) with change in numbers of inflowing fuel particles does not influence the model predictions significantly. However, increasing the number of fuel particles added every step leads to an increase in the total number of particles within the system and consequently a higher computational cost. Therefore, in the following numerical simulation, the number of fuel particles added per time step during fuel injection N_{f} was set to 1. Since the quantity of fresh air is always more than it required (for lean operation), the number of fresh air particles added every step, N_{a}, was set to 1 as well (the weight of fresh air particle equals its mass).

Next, we evaluate the sensitivity of the model prediction to the parameters associated with the down-sampling technique.

4.2 Determination of down-sampling parameters

The down-sampling algorithm contains two parameters, the number of conserved scalars $ns + 1$ and the number of particles n. In this section, the influence of

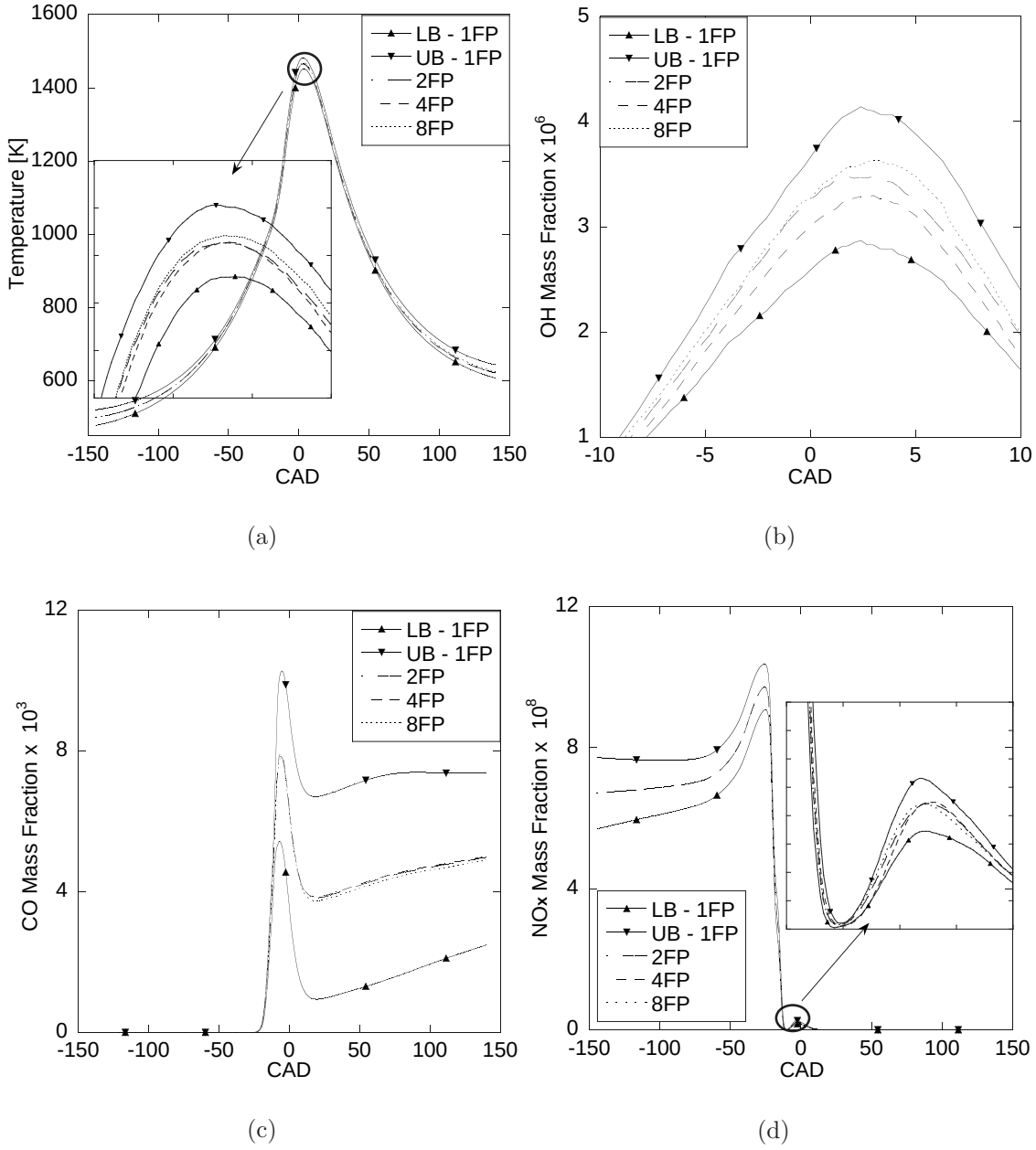

Figure 1: *Effect of the number of fuel particles added during inflow-outflow on the properties of the mixture in the partially mixed case ($\tau_{\mathrm{m}} = 2.0 \times 10^{-2} s$): (a) temperature, (b) OH mass fraction, (c) CO mass fraction, (d) NO_x mass fraction. Here, LB and UB denote lower bound and upper bound respectively, and FP denotes the number of inflowing fuel particles per time step.*

these parameters on the statistical and systematic errors is studied and then the appropriate down-sampling parameters are determined. In order to study the error incurred exclusively by the down-sampling process, the stochastic heat transfer submodel was switched off. Thus, the down-sampling procedure is the sole source of the statistical error. Furthermore, the partially mixed case was studied particularly due to its high standard deviation.

In the particle method, the macroscopic properties are calculated by averaging over all particles at each point in time. In order to estimate the random fluctuations of the down-sampling algorithm, L repetitions were performed. The corresponding values of the macroscopic properties are denoted by $\zeta^{(n,1)}(t), ..., \zeta^{(n,L)}(t)$, where n is the number of particles after down-sampling.

The empirical mean value of the macroscopic properties is

$$\eta_1^{(n,L)}(t) = \frac{1}{L}\sum_{l=1}^{L} \zeta^{(n,l)}(t),$$

and the empirical variance of the macroscopic properties is

$$\eta_2^{(n,L)}(t) = \frac{1}{L}\sum_{l=1}^{L} \left[\zeta^{(n,l)}(t)\right]^2 - \left[\eta_1^{(n,L)}(t)\right]^2.$$

The statistical error is the difference between the empirical mean value and the expected value of the macroscopic properties. The statistical error is defined as

$$C_{\text{stat}} = \max_i \left\{ \alpha_p \sqrt{\frac{\eta_2^{(n,L)}(t_i)}{L}} \right\}, \qquad t_i \leqslant t_{\text{stop}},\ t_i = i\Delta t,\ i \geqslant 0,$$

where $\alpha_p = 3.29$ is used for a confidence level of $p = 0.999$.

The systematic error is the difference between the expectation of the macroscopic properties and the exact value of the functional. In this study, the base case, i.e. the simulation without down-sampling, is used as the reference solution $F(t)$. Thus, a measure of the systematic error is defined as

$$C_{\text{sys}} = \max_i \left\{ \left| \eta_1^{(n,L)}(t_i) - F(t_i) \right| \right\}.$$

Asymptotically (i.e. for $L \to \infty$), the statistical error is inversely proportional to $\sqrt{L}$. To determine an appropriate number of repetitions, two set of simulations, one with 10 and the other with 80 repetitions, were compared. For these two cases 10 species were conserved. A detailed comparison is given in Table 2.

From Table 2, it can be observed that the statistical error scales inversely to $\sqrt{L}$ and the error is sufficiently small at $L = 10$ to keep the number of repetitions at that value in the remainder of this section.

In Table 3, the systematic and the statistical errors for the number of particles, $n = 32$ and $n = 213$ are provided.

Table 2: *Comparison of statistical errors between the sets of simulation (L=10 and L=80)*

	OH	CO	NO_x	T [K]
$L_1 = 10$	6.16×10^{-8}	2.45×10^{-4}	1.29×10^{-9}	6.36
$L_2 = 80$	2.21×10^{-8}	8.62×10^{-5}	5.58×10^{-10}	2.22
$\frac{C_{\text{stat}}^{L_1}}{C_{\text{stat}}^{L_2}} \times \frac{\sqrt{L_1}}{\sqrt{L_2}}$	0.985	1.0	0.817	1.01

Table 3: *Comparison of statistical errors and systematic errors*

ns=10, n=32

	OH	CO	NO_x	T [K]
C_{stat}	8.98×10^{-8}	3.31×10^{-4}	2.14×10^{-9}	9.22
C_{sys}	6.55×10^{-8}	7.49×10^{-5}	1.25×10^{-9}	2.53

ns=10, n=213

	OH	CO	NO_x	T [K]
C_{stat}	1.01×10^{-8}	1.09×10^{-4}	3.56×10^{-10}	1.62
C_{sys}	7.15×10^{-9}	2.31×10^{-5}	3.82×10^{-10}	0.66

These data indicate that the statistical error is generally larger than the systematic error. Therefore, in the next part we will only focus on the statistical error.

Next, we conducted a series of six simulations: Case (a) to Case (d) where 9, 19, 39, and 79 species were conserved respectively. Case (e) denotes the simulation run conserving just the four elements (C, H, O, N). In all the cases the total enthalpy was conserved, while the number of particles after down-sampling varied from 13 to 233. Case (f) was performed without conserving any properties and the number of particles was varied as 10, 20, 45, 95 and 200. The comparison of statistical errors associated with the species OH, CO, NO_x, and the temperature, T between these simulations is shown in Figure 2. It can be observed that the statistical error for OH, NO_x, and T scales inversely with the number of particles, whereas that for CO is inversely proportional to $\sqrt{n}$. This difference could arise from the correlation of the scalar properties for different particles. Furthermore, the number of conserved species were not found to influence the error significantly. However, without conserving any species a significant error was incurred. Based on this study, it can be concluded that for the engine simulation with the given conditions, the Case (a) conserving 9 species with 50 particles retains adequate accuracy. Having studied the down-sampling parameters, we now consider multiple engine cycle simulations. Cycle simulations help in better understanding cyclic variation of the scalar properties and thereby devising variable control strategies for optimal engine performance and emissions.

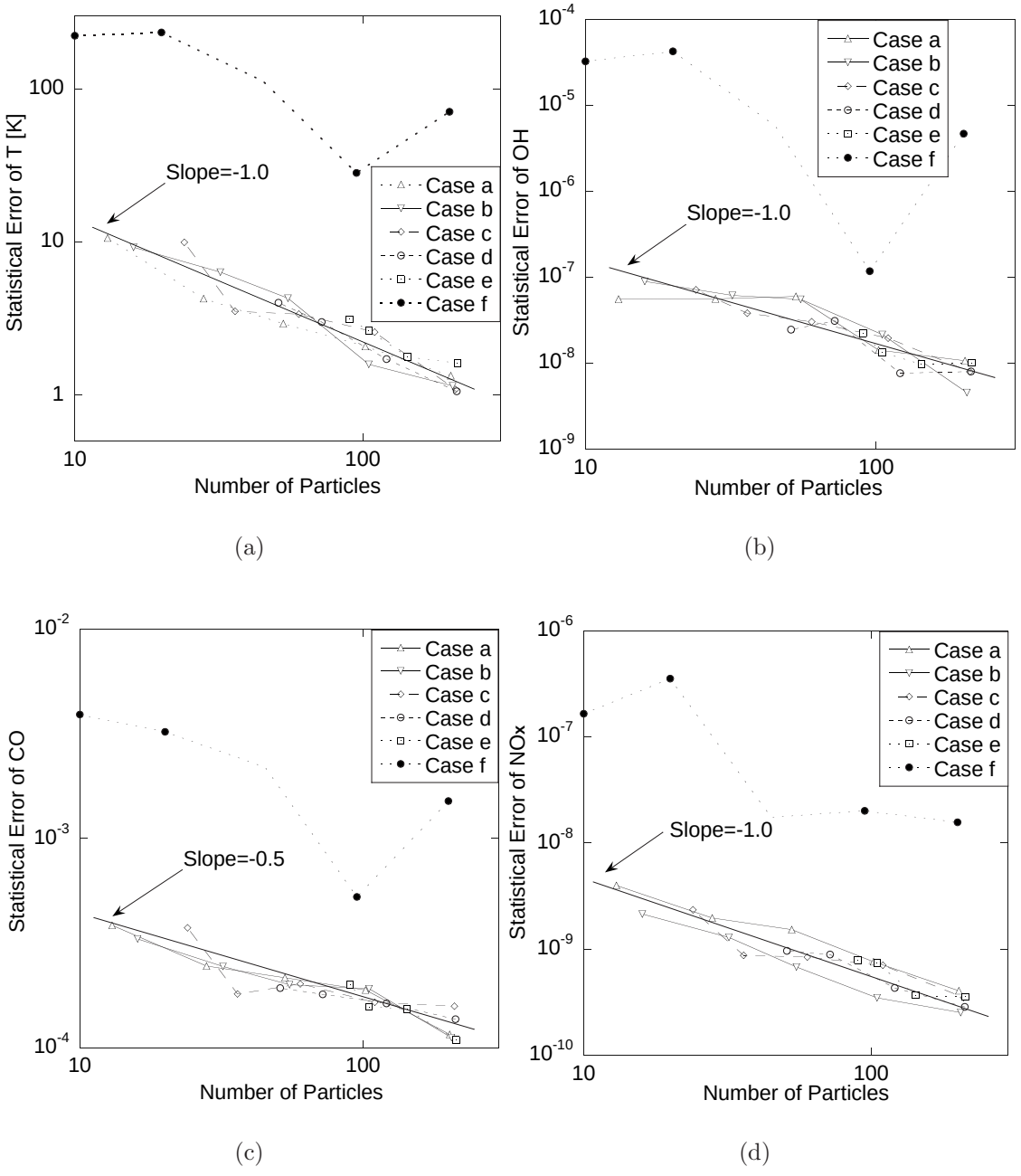

Figure 2: *Effect of the number of conserved species and the number of particles after down-sampling on the statistical errors of the mixture's properties in the partially mixed case: (a) temperature, (b) OH mass fraction, (c) CO mass fraction, (d) NO_x mass fraction.*

4.3 Multiple cycle simulation

In this section multi-cycle simulations are conducted to investigate the accumulation of error on account of the down-sampling during several engine cycles. Here, ns and n are set to 19 and 120 respectively. With the down-sampling strategy implemented, 10 successive engine cycles for both cases of characteristic mixing times were simulated. In this section and section 4.4, the method as described in section 4.1 (from eqn. (11) to eqn. (13)), is employed for data analysis.

Figure 3 to Figure 6 depict the effect of down-sampling on the temperature, and mass fractions of OH, CO and NO_x for the partially mixed case while Figures 7 to 10 denote the same for the well-mixed case. In these figures c denotes the engine cycle index. The higher initial temperature observed for the second cycle can be attributed to the initial condition for composition and temperature, without the steady state being reached. Particularly for the partially mixed case the confidence band for the 10^{th} cycle, especially for the chemical species (Figure 5 to Figure 6) are very wide indicating a large standard deviation. This is due to the fact that the species compositions are very sensitive to the system temperature, in other words, a slight temperature change results in a large mass fraction variation of OH, CO and NO_x. As compared to the partially mixed system, the simulation results for the well-mixed system show a much narrower confidence band on account of the greater homogeneity and hence lower standard deviation. Furthermore for the well-mixed system, the temperature, and mass fractions of OH, CO from the third to ninth cycles lie within the confidence bands of the tenth cycle. However, the profile for the NO_x mass fraction lies outside the confidence band of the last cycle. For example, from Figure 11, it can be seen that the NO_x confidence band of the 10^{th} cycle does not overlap with those from the 6^{th} and 7^{th} cycles. This behaviour probably arises from the high sensitivity of NO_x to the temperature and the fluctuations in the system. However, there is no evidence for an accumulated error with respect to the number of cycles.

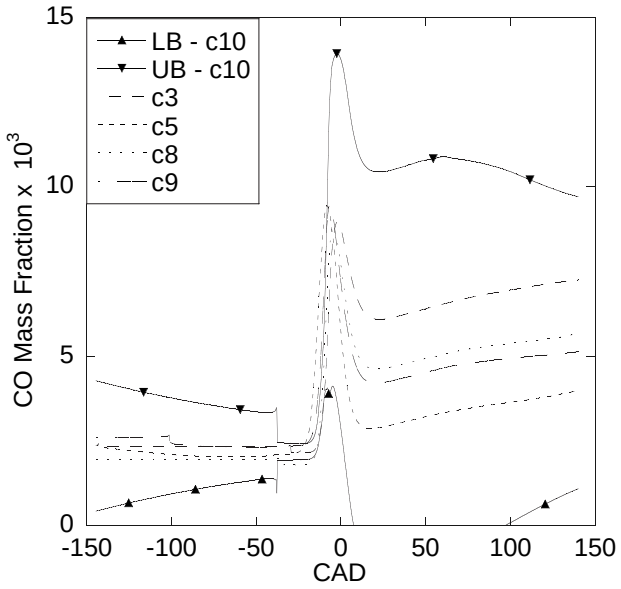

Figure 4: *Mean CO mass fraction for several engine cycles (Confidence bands plotted for the 10$^{\text{th}}$ cycle) in the partially mixed case.*

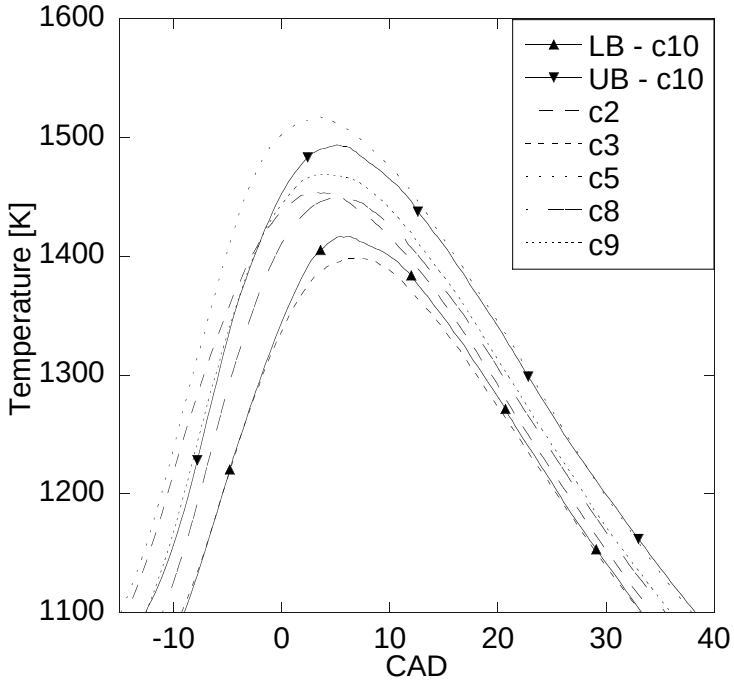

Figure 3: *Mean in-cylinder temperature for several engine cycles (Confidence bands plotted for the 10th cycle) in the partially mixed case. c denotes the engine cycle index.*

In conclusion, for both the well-mixed and partially-mixed case, the down-sampling did not accumulate noticeable errors for the multi-cycle simulations.

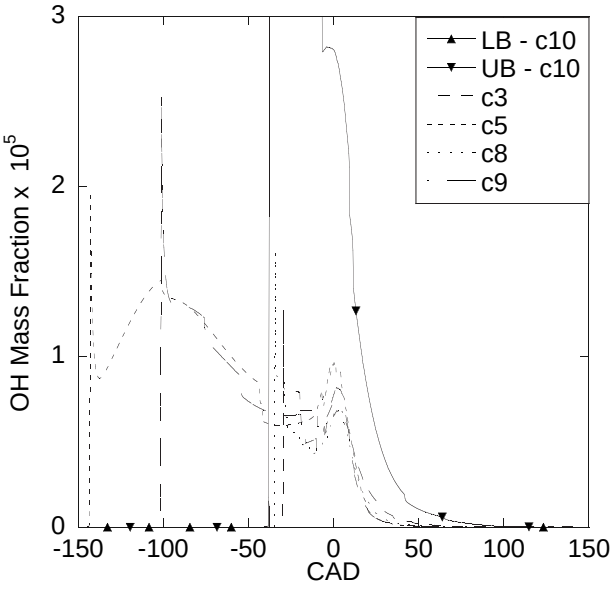

Figure 5: *Mean OH mass fraction for several engine cycles (Confidence bands plotted for the 10$^{\text{th}}$ cycle) in the partially mixed case.*

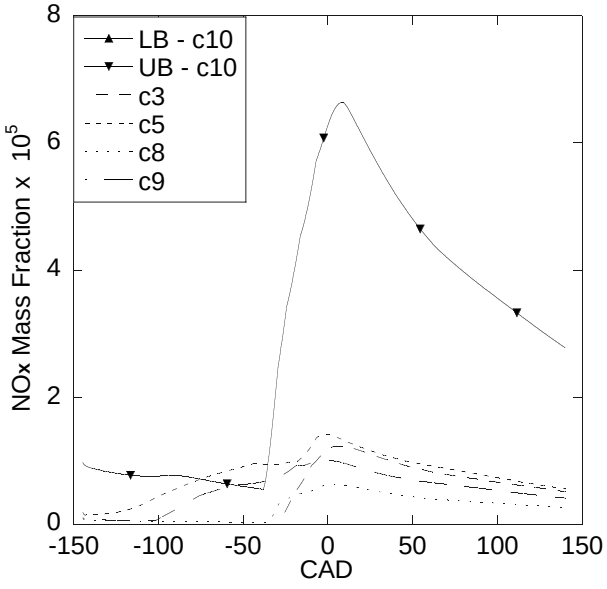

Figure 6: *Mean NO_x mass fraction for several engine cycles (Confidence bands plotted for the 10$^{\text{th}}$ cycle) in the partially mixed case.*

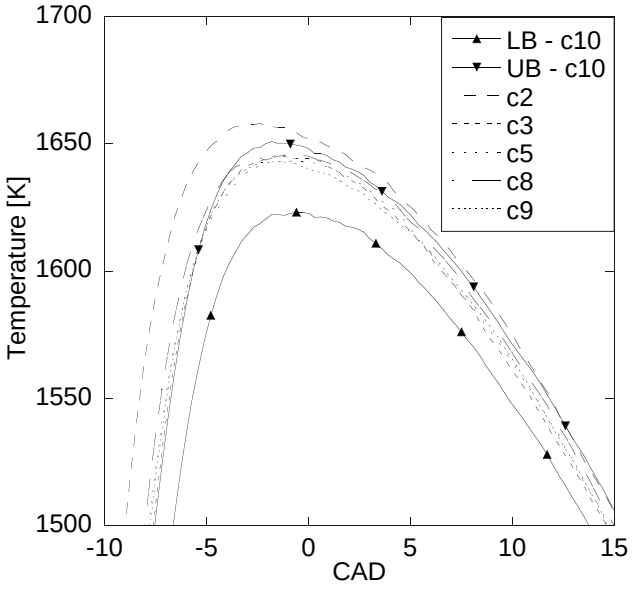

Figure 7: *Mean in-cylinder temperature for several engine cycles (Confidence bands plotted for the 10$^{\text{th}}$ cycle) in the well-mixed case.*

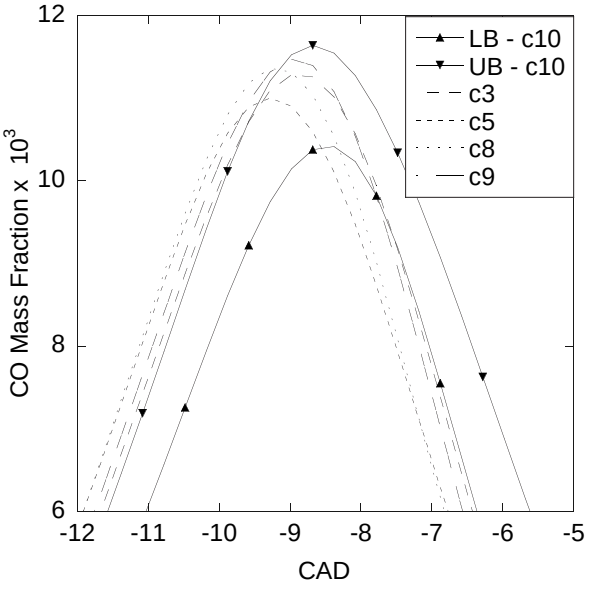

Figure 8: *Mean CO mass fraction for several engine cycles (Confidence bands plotted for the 10$^{\text{th}}$ cycle) in the well-mixed case.*

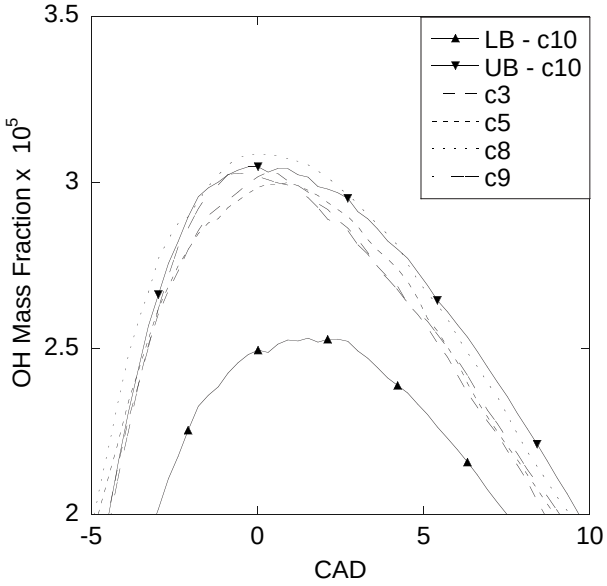

Figure 9: *Mean OH mass fraction for several engine cycles (Confidence bands plotted for the 10$^{\text{th}}$ cycle) in the well-mixed case.*

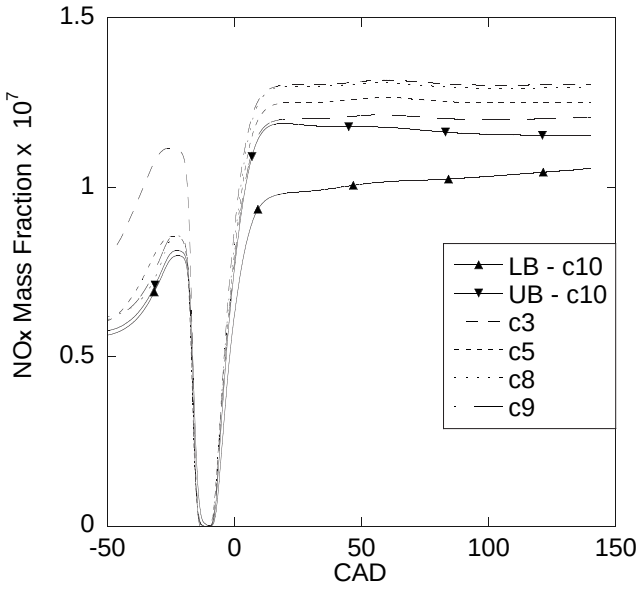

Figure 10: *Mean NO_x mass fraction for several engine cycles (Confidence bands plotted for the 10$^{\text{th}}$ cycle) in the well-mixed case.*

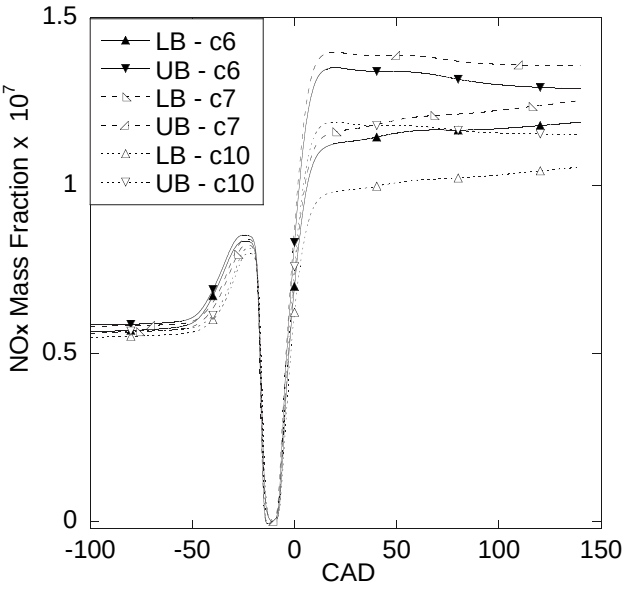

Figure 11: *The confidence band of the tenth-cycle NO_x mass fraction versus the 6^{th} and 7^{th} cycles in the well-mixed case.*

4.4 Down-sampling: efficiency gains

In order to evaluate the effect of the introduction of the down-sampling algorithm into the SRM-DI model the simulation results obtained with and without the down-sampling algorithm implemented were compared. Influence on the computational expense and the error caused by down-sampling for the partially mixed and well-mixed systems were also studied. We define the *down-sampling factor* M as the particle reduction ratio, i.e. $M := N/n$, where N and n are the number of particles before and after down-sampling respectively.

Figure 12 and Figure 13 summarize the simulated results for the partially mixed and well-mixed systems respectively. The results in both figures demonstrate that introducing the down-sampling strategy into the SRM-DI did not constitute a significant compromise of the accuracy of the simulation. The simulated results obtained with the down-sampling factor, 3 and 5 were nearly within the confidence band determined with $M = 1$ (i.e. base case). However, when M was increased, e.g. 9.3, the profiles of scalar variables overlapped with the confidence bands of the corresponding variables for the base case. Therefore, overall it can be concluded that the down-sampling procedure is acceptable in the simulation of a HCCI engine under given conditions, although larger down-sampling factors led to higher error.

Furthermore, the computational costs with and without down-sampling are compared and the results are listed in Table 4. It can be seen from Table 4 that within an acceptable error, the introduction of the down-sampling strategy can speed up the simulation approximately 8 times for both partially mixed and well-mixed systems.

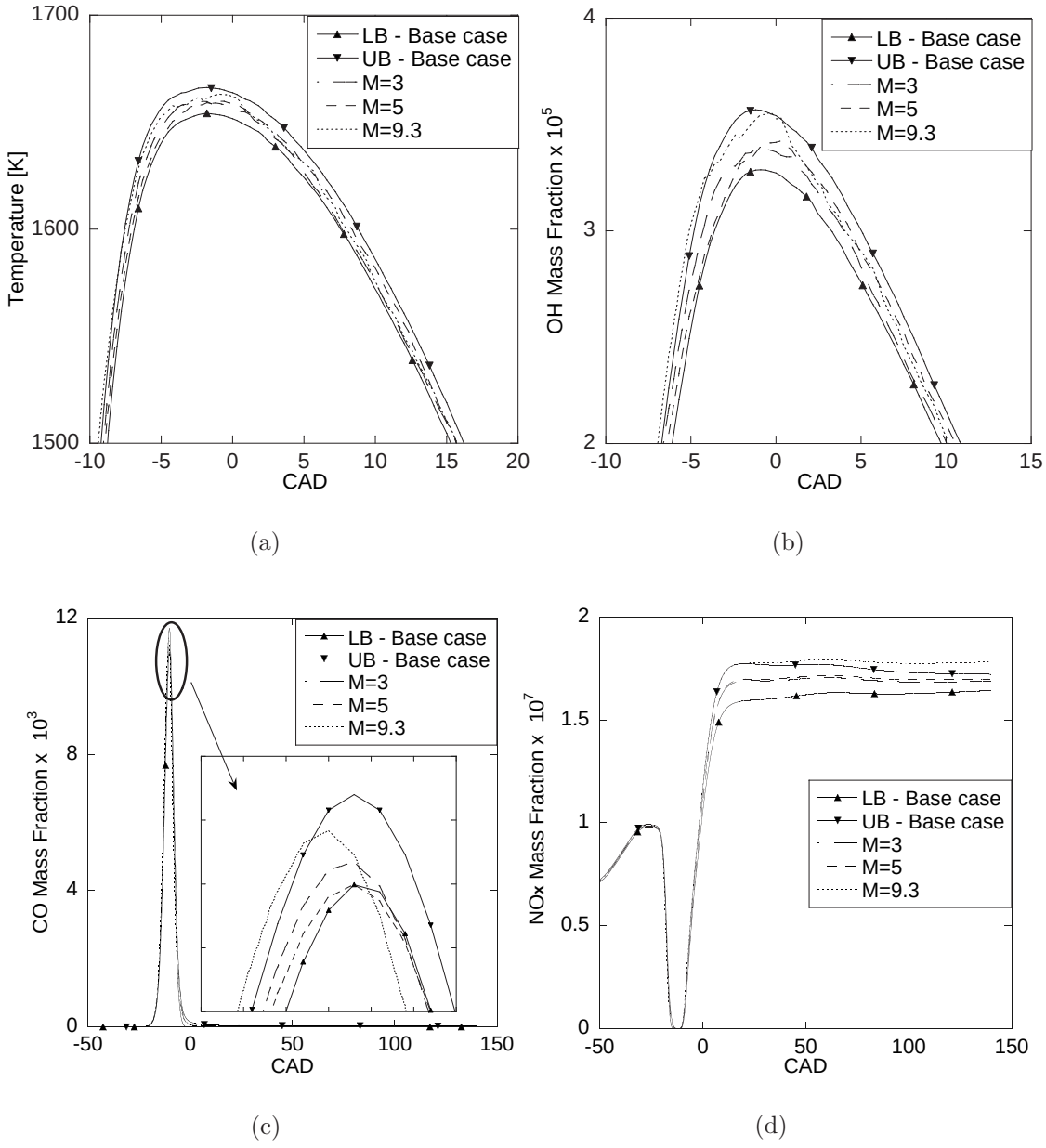

Figure 12: *Effect of the down-sampling on the simulated properties of the gas mixture in the well-mixed case ($\tau_{\mathrm{m}} = 2.0 \times 10^{-4} s$) : (a) temperature, (b) OH mass fraction, (c) CO mass fraction, (d) NO_x mass fraction.*

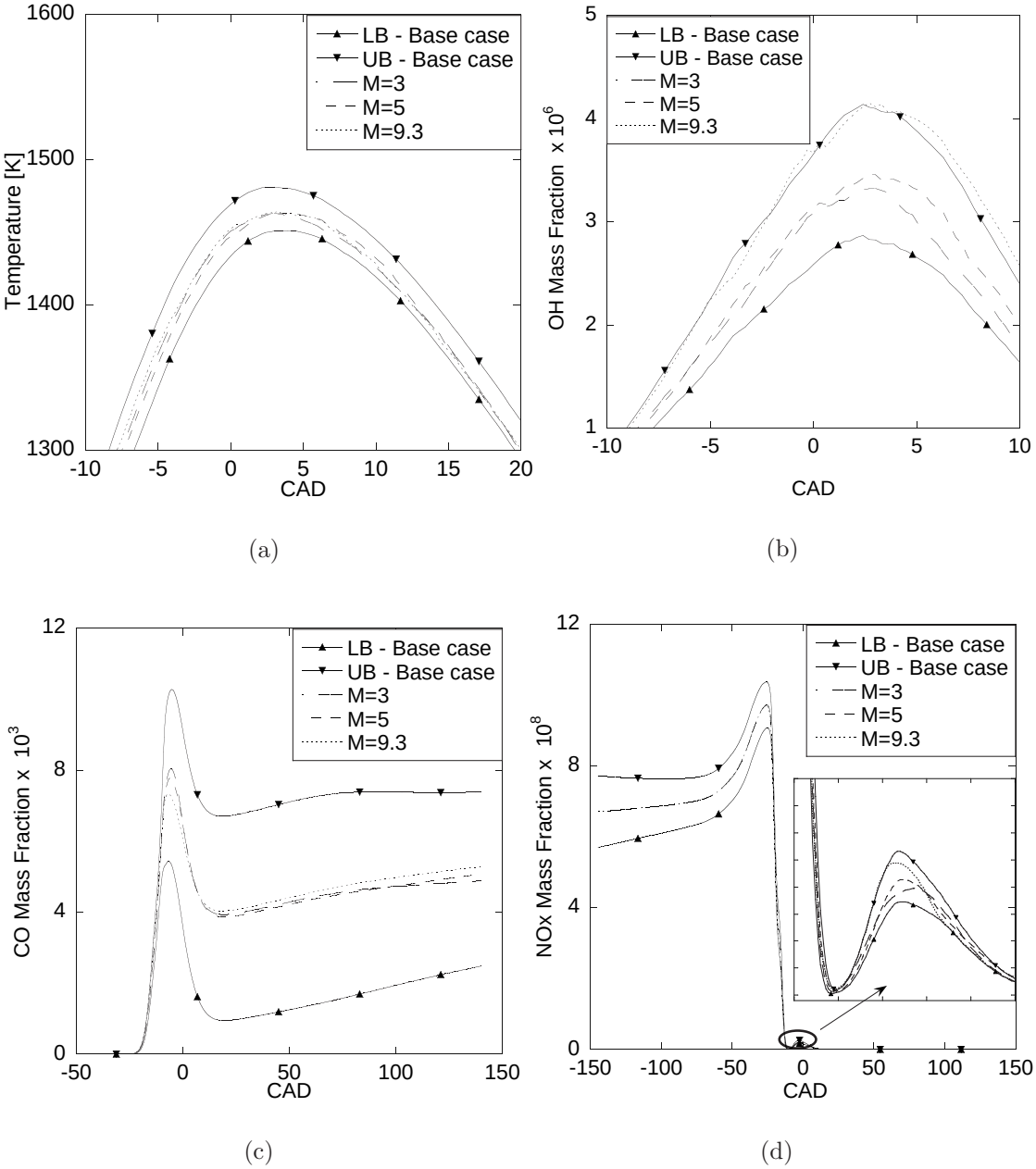

Figure 13: *Effect of the down-sampling on the simulated properties of the gas mixture in the partially mixed case ($\tau_{\mathrm{m}} = 2.0 \times 10^{-2} s$) : (a) temperature, (b) OH mass fraction, (c) CO mass fraction, (d) NO_x mass fraction.*

Table 4: *The comparison of computational time for well-mixed and partially mixed systems*

		CPU Time (mins)	
Simulation Case	Factor M	$\tau_{\mathrm{m}} = 2 \times 10^{-2} s$	$\tau_{\mathrm{m}} = 2 \times 10^{-4} s$
Base Case($N = n = 334$)	1	705	252
Down-sampling($n = 111$)	3	237	86
Down-sampling($n = 66$)	5	138	47
Down-sampling($n = 36$)	9.3	83	30

In the next section, the model is used to predict the effect of engine parameters on HCCI combustion and emissions.

5 Effects of Relative Air-fuel Ratio and Injection Timing on Combustion

In order to control HCCI engine operation, several approaches have been investigated, for example, changing relative air-fuel ratio, injection timing, IVO timing, EVC timing, engine speed, boost pressure, intake gas temperature etc. as well as hybrid methods involving the integration of these strategies. With the current development of the SRM-DI model, not all mentioned strategies can be investigated in this work. We focus on evaluating the effect of two specific engine strategies, namely, varying relative air-fuel ratio and direct injection timing. For studying these two parameters, the model predictions will be compared with the experiment data qualitatively. As compared to the partially mixed case, the well-mixed case provides a better representation of the volume averaged mixing time (obtained from CFD calculations) for the two-stroke engine operation considered here. Hence, the well mixed case is chosen for the engine parametric studies in the next section.

5.1 Relative air-fuel ratio

HCCI combustion ignition is influenced by the temperature, the pressure and the species mass fractions of the mixture in the cylinder. The strategies of varying relative air-fuel ratio (λ) influence the fuel concentration directly. Generally, this technique is integrated with injection timing, injection method, EGR valve timing, engine speed etc. to operate the HCCI engine.

In this section, HCCI combustion with early single-stage injection was investigated while relative air-fuel ratio was varied from 2.3 to 5.6. The results are shown in Figure 14.

It can be observed that as λ decreases, the peak temperature, the peak pressure, the mass fraction of NO_x increase while CO mass fraction decreases. When λ reaches

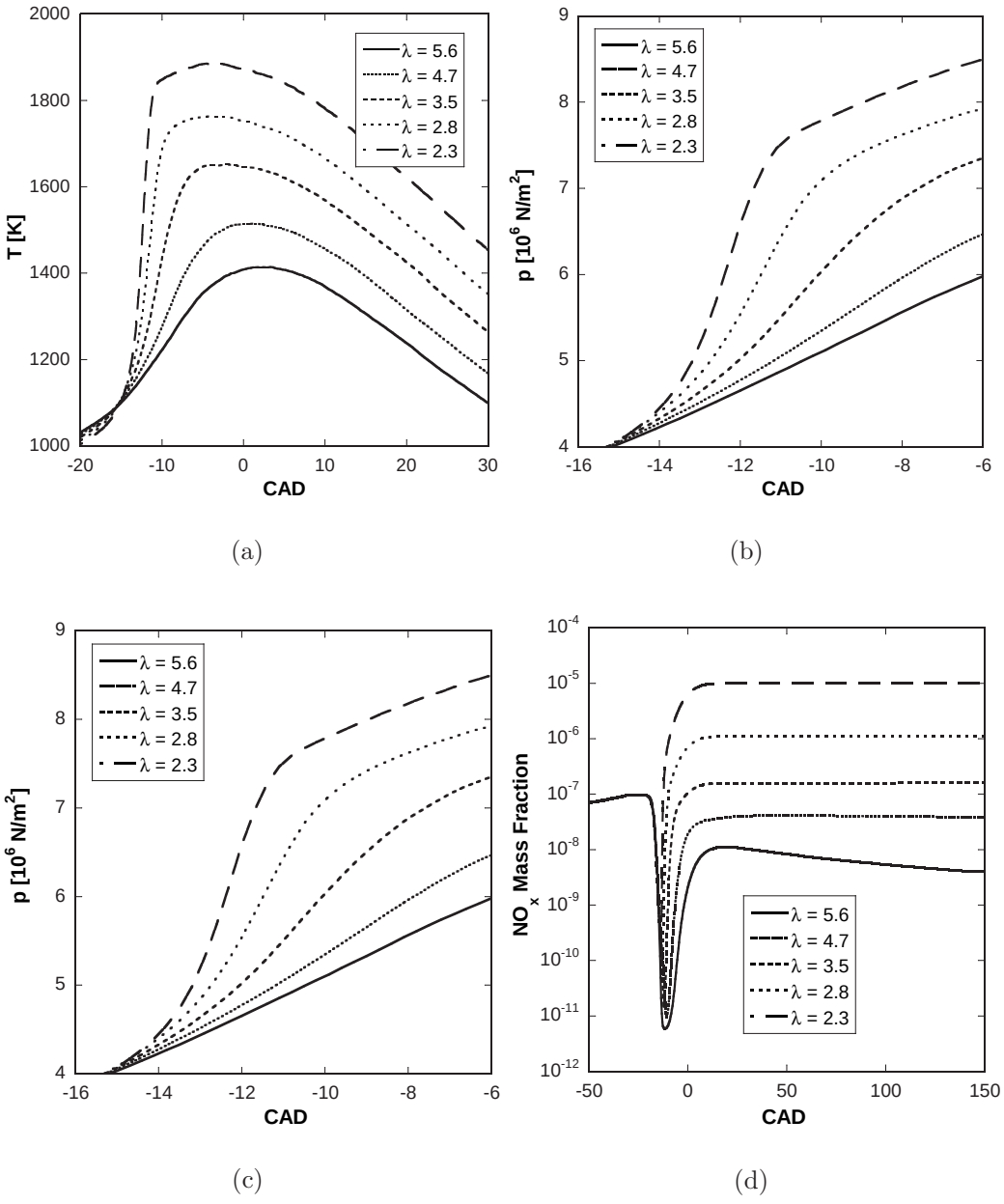

Figure 14: *Effect of the air-fuel ratio on the mixture's properties in the well-mixed case: (a) temperature, (b) pressure, (c) CO mass fraction, (d) NO_x mass fraction.*

to 2.3, the maximum pressure gradient is higher than 15 bar/CAD, this could cause engine knock and high NO_x emissions. On the other hand, when λ is too high, i.e. fuel is too lean, and hence, the mixture can not be burnt completely. It leads to high CO concentration. These trends match well with the experimental data in ref. (Urushihara et al., 2003; Wang et al., 2005).

5.2 Direct injection timing

In this section, the effect of varying SOI is studied. As the injection is well before TDC the mixture is almost homogeneous before the ignition is triggered.

Figure 15 shows that for the range of injection timings chosen the properties of the mixture do not vary significantly. For example, for the cases with SOI 170 CAD and 180 CAD, the profiles for the scalar properties overlap. This is due to greater homogeneity for these two cases. Later injection (SOI equals 190 CAD and 200 CAD) causes relatively more inhomogeneity and results in a slightly higher peak temperatures and NO_x mass fraction. This predicted trend matches the experimental observations by Sjöberg et al. (Sjöberg et al., 2002).

To study the effect of late direct injection, a more sophisticated treatment of the mixing than what the IEM model provides is necessary. In particular localness of the scalars needs to be accounted for. However, the new SRM-DI model qualitatively predicted the effects of variation in the relative air-fuel ratio and the **early** direct injection timing on HCCI combustion and emissions.

6 Conclusions

A novel SRM-DI model based on the probability density function (PDF) approach was formulated to simulate a direct injection HCCI engine operation. With the incorporation of the gas exchange processes, the computational expense increased rapidly. Hence, a conservative down-sampling procedure combined with a weighted-particle Monte Carlo method was developed to reduce the number of particles while conserving the statistical properties of the ensemble.

A systematic numerical investigation of the model performance with respect to the various numerical parameters was carried out. It was observed that the algorithm was more sensitive to the number of particles than the number of conserved chemical species. Furthermore, multiple cycle simulation studies demonstrated that the error due to down-sampling was not accumulated with respect to the number of engine cycles. Additionally, implementing the down-sampling technique in an engine cycle simulation resulted in a speed-up by a factor of 8, without incurring significant error in the numerical solution.

Model predictions for the effects of varying the relative air-fuel ratio and direct injection timing on HCCI combustion and emissions agreed with the qualitative

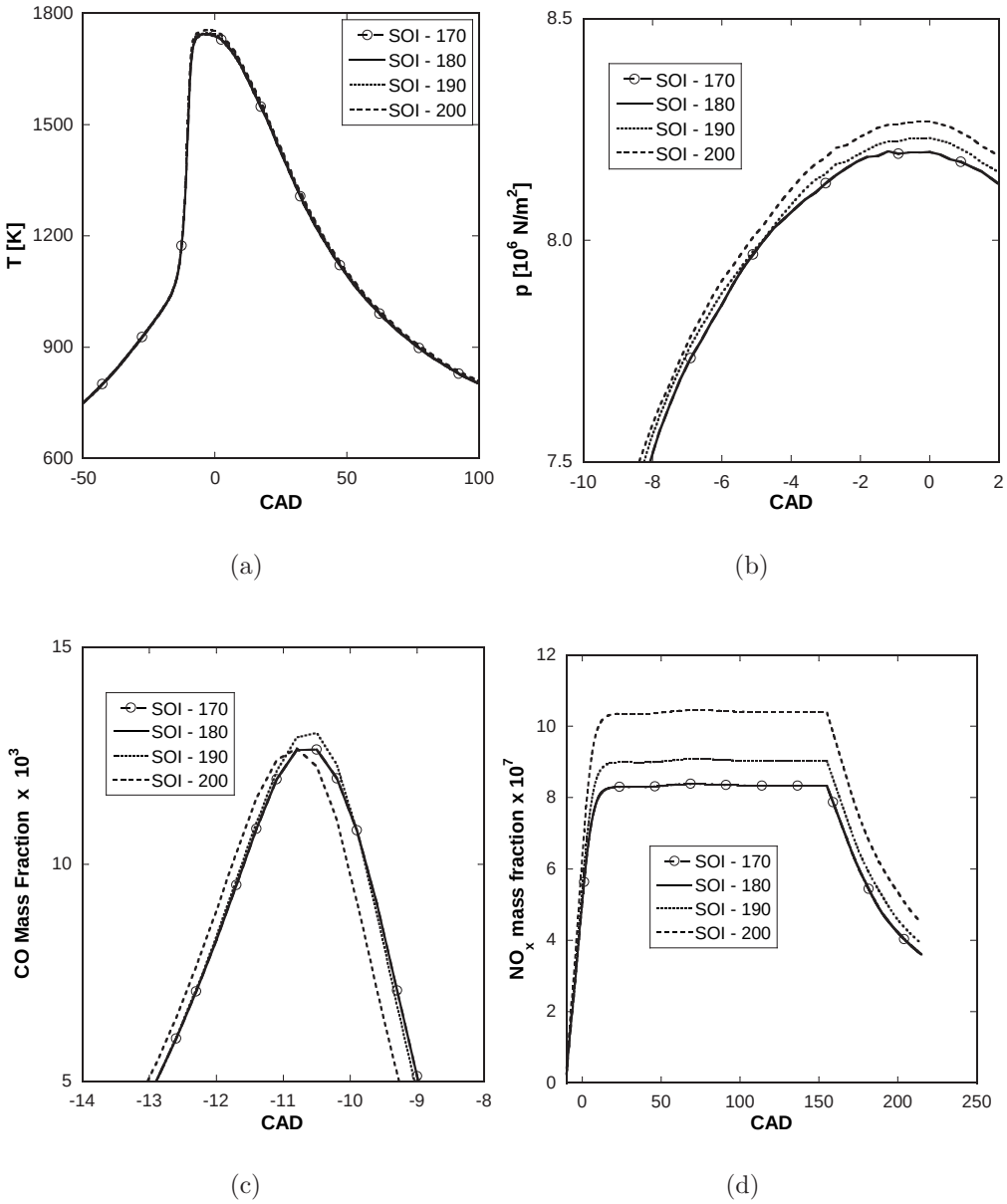

Figure 15: *Effect of the early direct injection timing on the mixture's properties in the well-mixed case: (a) temperature, (b) pressure, (c) CO mass fraction, (d) NO_x mass fraction.*

trends observed in measurements elsewhere.

The framework built here can now be used to formulate an advanced model for simulating multiple and late direct injection HCCI combustion. Currently the efforts are being focussed at developing detailed sub-models for spray injection and turbulent mixing to improve the predictive power of the model.

A Appendix

Consider an ensemble of particles which are characterized by the $s+1-$dimensional vector of internal parameters $\psi = (\psi^{(1)}, \psi^{(2)}, ..., \psi^{(s+1)})$, where $\psi^{(i)}$ can be mass, momentum or energy of the particle or mass of a chemical component which the particle contains. The ensemble is described by the mass density function $\mathcal{F}(\psi) = \rho(\psi)f(\psi)$. Throughout this section, we drop the time dependencies from all the notations.

The main idea of the Monte Carlo method is the representation of the ensemble of a large number of the physical particles by an ensemble of relatively small number N of the computational particles such that a group of W identical molecules or particles in the physical system is substituted by one computational particle. The parameter $W^{(i)}$ is the statistical weight of the i^{th} computational particle. In other words the function $\mathcal{F}(\psi)$ is replaced by a weighted sum of delta function as given in eqn. (7)

Usually, the Monte Carlo method is used for estimation of the following linear functionals

$$Z(\mathcal{F}(\psi)) = \int \mathcal{F}(\psi)z(\psi)d\psi \approx \sum_{i=1}^{N} W^{(i)}z(\psi^{(i)}), \tag{14}$$

where $z(\psi)$ is an integrable function. Generally speaking, the estimation (14) is a random variable and varies from one run of the Monte Carlo algorithm to other, but some of them such as mass, momentum and energy are conserved variables and remain constant. If a Monte Carlo algorithm does not conserve these values it suffers from large unphysical oscillations. The proposed algorithm aims to avoid this situation.

As the number of particles in the system becomes too large, some of them have to be removed and their statistical weights to be redistributed over the remaining particles. Our purpose is to construct an algorithm that keeps the distribution function (eqn. (7)) statistically intact and also conserves physically important statistical moments. Below we describe the restrictions which have to be imposed on such transformations.

First of all, the statistical weights are always non-negative:

$$W^{(i)} \geqslant 0. \tag{15}$$

In order to formulate the second condition define ns statistically important functionals $Z_j(\mathcal{F}(\psi)) = \int \mathcal{F}(\psi)z_j(\psi)d\psi$, where $j = 1, \ldots, ns$. Any redistribution of the

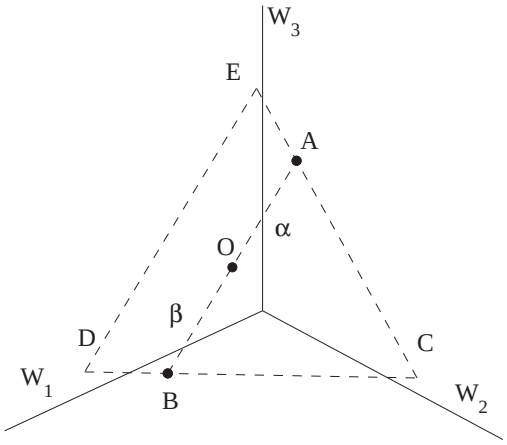

Figure 16: *Schematic view of the down-sampling algorithm, the dimension of the space $N = 3$ and the number of the constraints (16) is $ns = 1$.*

statistical weights cannot affect the estimation (14). Thus $W^{(i)}$ satisfy the system of linear equalities:

$$\sum_{i=1}^{N} z_j(\psi^{(i)})W^{(i)} = \sum_{i=1}^{N} \Pi_{ji} W^{(i)} = Z_j \tag{16}$$

We also require that the statistical weights are bounded from above:

$$W^{(i)} \leqslant W_{\max}. \tag{17}$$

This condition is not necessary for the method described below, but the presence of few particles with large statistical weights means that the estimation (14) is based on these particles mainly, while the contribution of the rest of the particles is negligible. In this case the Monte Carlo method suffers from large statistical error.
Eqs. (15)-(17) imply that the vector W of the statistical weights belongs to a $(N - ns)$-dimensional convex polygon as it schematically shown on Fig. 16. If $0 < W^{(i)} < W_{\max}$ then W belongs to the interior of the polygon, while the edges of the polygon correspond either to $W^{(i)} = 0$ or $W^{(i)} = W_{\max}$. An interior point of the convex polygon O can be represented as a linear combination of two points that belong to the edges:

$$O = pA + (1 - p)B,\ 0 < p < 1.$$

Interpretation of p in the above equation as a probability yields the algorithm for the reduction of the number of particles:

1. Generate a uniformly distributed unit vector g.

2. We want to replace the vector W by $W = W + bg$, where b is a scalar. Thus, in order to satisfy Eq. (16) the vector g has to be orthogonal to the subspace formed by the columns of the matrix Π. Thus we recalculate g as

$$g := g - \Pi(\Pi^T\Pi)^{-1}\Pi^T g.$$

   Direct calculation shows that after this transformation $\Pi^T g = 0$.

3. Find

$$\alpha = \min\left\{\min_{g^{(i)}<0}\{-\frac{W^{(i)}}{g^{(i)}}\},\ \min_{g^{(i)}>0}\{\frac{W_{\max}-W^{(i)}}{g^{(i)}}\}\right\}.$$

4. Find

$$\beta = \min\left\{\min_{g^{(i)}>0}\{\frac{W^{(i)}}{g^{(i)}}\},\ \min_{g^{(i)}<0}\{\frac{W^{(i)}-W_{\max}}{g^{(i)}}\}\right\}.$$

5. With probability $\beta/(\alpha+\beta)$ choose the point A, i.e., replace the vector W by $W = W + \alpha g$.

6. Otherwise choose the point B: $W = W - \beta g$.

After one iteration of the above algorithm, Eq. (14) becomes:

$$Z_1(\mathcal{F}(\psi)) \approx \sum_{i=1}^{N}(W^{(i)} + \alpha g^{(i)})z(\psi^{(i)}),$$

with probability $\beta/(\alpha+\beta)$, or

$$Z_2(\mathcal{F}(\psi)) \approx \sum_{i=1}^{N}(W_i - \beta g_i)z(\psi^{(i)})$$

with probability $\alpha/(\alpha+\beta)$. Direct calculation shows that

$$\langle Z(\mathcal{F}(\psi))\rangle = \frac{\beta}{\alpha+\beta}Z_1(\mathcal{F}(\psi)) + \frac{\alpha}{\alpha+\beta}Z_2(\mathcal{F}(\psi)) = Z(\mathcal{F}(\psi))$$

and the estimation (14) remains statistically intact for arbitrary $z(\psi)$, while the statistical weights of one of the particles is either 0 or $W_{\max}$.

We repeat this procedure $N - ns$ times until the algorithm reaches a corner point of the polygon, i.e., if we choose the point A then at the next iteration we choose randomly between the points C and E, while if we choose the point B then we have to choose between the points C and D. The performance of the proposed algorithm is illustrated on Fig. 17. We randomly generated an ensemble of $N = 100$ particles which consist of 6 components, the masses of the components in a particle are uniformly distributed from 0 to 1. As one can see, only 6 particles have weights between 0 and 5 that corresponds to the number of the conserved scalars. Creation of a particle with weight $W_{\max}$ has to be balanced by removal of $W_{\max} - 1$ other particles, since in the present case $W_{\max} = 5$, the number of the particles with weight $W_{\max}$ is to the number of the particles with weight 0 as $17/77 \approx 1/5$.

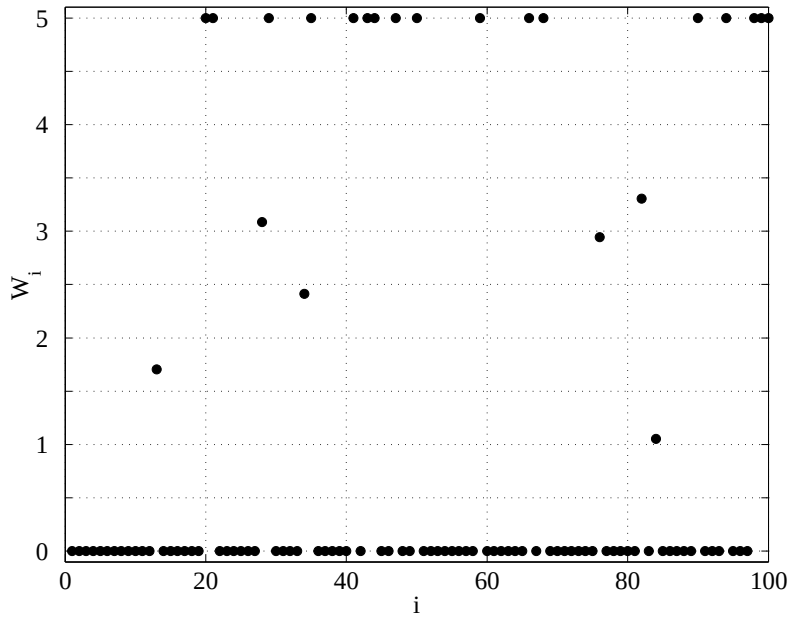

Figure 17: *Statistical weights of an ensemble of* $N = 100$ *particles after the down-sampling. Initial statistical weights are* $W^{(i)} = 1,\ i = 1, \ldots, N$, $W_{\max} = 5$ *and the number of the constraints (16) is* $ns = 6$.

References

A. Bhave, M. Balthasar, M. Kraft, and F. Mauss. Analysis of a natural gas fuelled homogeneous charge compression ignition engine with exhaust gas recirculation using a stochastic reactor model. *Int. J. Engine Res.*, 5(1):93–103, 2004a.

A. Bhave and M. Kraft. Partially stirred reactor model: Analytical solutions and numerical convergence study of a PDF/Monte Carlo method. *SIAM J. Sci. Comput.*, 25(5):1798–1823, 2004.

A. Bhave, M. Kraft, F. Mauss, A. Oakley, and H. Zhao. Evaluating the EGR-AFR operating range of a HCCI engine. *SAE paper, No. 2005-01-0161*, 2005.

A. Bhave, M. Kraft, L. Montorsi, and F. Mauss. Modelling a dual-fuelled multi-cylinder HCCI engine using a PDF-based engine cycle simulator. *SAE paper, No. 2004-01-0561*, 2004b.

J. Y. Chen. Stochastic modeling of partially stirred reactors. *Combust. Sci. and Tech.*, 122:63–94, 1997.

S. M. Correa and M. E. Braaten. Parallel simulations of partially stirred methane combustion. *Combust. Flame*, 94:469–486, 1993.

M. Guenthner, W. Sauter, F. Schwarz, A. Velji, and U. Spicher. A study of the ignition and combustion process in a gasoline HCCI engine using port and direct fuel injection. *6th International Symposium on Diagnostics and Modeling of Combustion in Internal Combustion Engines (COMODIA) 2004, Yokohama, Japan*, 2004.

R. Hasegawa and H. Yanagihara. Development of ignition control in HCCI DI diesel engine. *SAE paper, No. 2003-01-0745*, 2003.

R. Jhavar and J. Christopher. Effects of mixing on early injection diesel combustion. *SAE paper, No. 2003-01-0154*, 2005.

M. Kraft, P. Maigaard, F. Mauss, M. Christensen, and B. Johansson. Invesitigation of comubstion emissions in a homogeneous charge compression injection engine: Measurements and a new computational model. *Proc. Combust. Inst.*, 28: 11951201, 2000.

B. Leach, H. Zhao, Y. Li, and T. Ma. Control of CAI combustion through injection timing in a GDI engine with an air-assisted injector. *SAE paper, No. 2005-01-0134*, 2005.

G. Lechner, T. Jacobs, C. Chryssakis, D. Assanis, and R. Siewert. Evaluation of a narrow spray cone angle, advanced injection timing strategy to achieve partially premixed compression ignition combustion in a diesel engine. *SAE paper, No. 2005-01-0167*, 2005.

P. Maigaard, F. Mauss, and M. Kraft. Homogeneous charge compression ignition engine: A simulation study on the effects of inhomogeneities. *J. Eng. Gas Turbines Power*, 125:466–471, 2003.

K. Narayanaswamy, R.P Hessel, and C. J. Rutland. A new approach to model DI-diesel HCCI combustion for use in cycle simulation studies. *SAE paper, No. 2005-01-3743*, 2005.

K. Narayanaswamy and C. J. Rutland. Cycle simulation diesel HCCI modelling studies and control. *SAE paper, No. 2004-01-2997*, 2004.

Y. Nishijima, Y. Asaumi, and Y. Aoyagi. Impingement spray system with direct water injection for premixed lean diesel combustion control. *SAE paper, No. 2002-01-0109*, 2002.

S. B. Pope. PDF methods for turbulent reactive flows. *Prog. Energy Combust. Sci.*, 11:119–192, 1985.

Y. Ra and R. D. Reitz. The use of variable geometry sprays with low pressure injection for optimization of diesel HCCI engine combustion. *SAE paper, No. 2005-01-0148*, 2005.

M. Sjöberg, L. Edling, T. Eliassen, L. Magnusson, and H. Angström. GDI HCCI: Effects of injection timing and air swirl on fuel stratification, combustion and emissions formation. *SAE paper, No. 2002-01-0106*, 2002.

R. Standing, N. Kalian, T. Ma, H. Zhao, M. Wirth, and A. Schamel. Effects of injection timing and valve timings on CAI operation in a multi-cylinder DI gasoline engine. *SAE paper, No. 2005-01-0132*, 2005.

G. Strang. On the construction and comparison of difference schemes. *SIAM J. Numer. Anal.*, 5(3):506–517, 1968.

W. Su, H. Wang, and B. Liu. Injection mode modulation for HCCI diesel combustion. *SAE paper, No. 2005-01-0117*, 2005.

F. Tao, Y. Liu, B. RempelEwert, D. Foster, R. Reitz, D. Choi, and P. Miles. Modeling the effects of EGR and injection pressure on soot formation in a high-speed direct-injection (HSDI) diesel engine using a multi-step phenomenological soot model. *SAE paper, No. 2005-01-0121*, 2005.

T. Tomoda, M. Kubota, R. Shimizu, and Y. Nomura. Numerical analysis of mixture formation of a direct injection gasoline engine. *5th International Symposium on Diagnostics and Modeling of Combustion in Internal Combustion Engines (COMODIA) 2001, Nagoya, Japan*, 2001.

T. Urushihara, K. Hiraya, A. Kakuhou, and T. Itoh. Expansion of HCCI operating region by the combination of direct fuel injection, negative valve overlap and internal fuel reformation. *SAE paper, No. 2003-01-0749*, 2003.

A. Vikhansky and M. Kraft. Conservative method for the reduction of the number of particles in the Monte Carlo simulation method for kinetic equations. *J. Comput. Phys.*, (203):371–378, 2005.

Z. Wang, J. Wang, S. Shuai, and Q. Ma. Effects of spark ignition and stratified charge on gasoline HCCI combustion with direct injection. *SAE paper, No. 2005-01-0137*, 2005.

B. Yang and S. B. Pope. An investigation of the accuracy of manifold methods and splitting schemes in the computational implementation of combustion chemistry. *Combust. Flame*, 112:16–32, 1998.

F. Zhao, T. Asmus, D. Assanis, J. Dec, J. Eng, and P. Najt. *Homogeneous Charge Compression Ignition (HCCI) Engines Key Research and Development Issues.* Society of Automotive Engineers,U.S., 2003. ISBN 076801123X.

Acknowledgement

We express our sincere thanks to Toyota Motor Co. Japan for providing the financial support for the research work. Authors (HS and AB) would also like to thank the Centre for Scientific Enterprise Limited (CSEL) for the fellowship-funding. Thanks are due to our colleagues at the Computational Modelling Group, University of Cambridge for their help with the manuscript.